Spontaneous Assembly of Perfectly Ordered Identical-Size Nanocluster Arrays

Jian-Long Li,[1] Jin-Feng Jia,[1] Xue-Jin Liang,[1] Xi Liu,[1] Jun-Zhong Wang,[1] Qi-Kun Xue,[1] Zhi-Qiang Li,[2] John S. Tse,[2] Zhenyu Zhang,[1,3] and S. B. Zhang[4]

[1]*State Key Laboratory for Surface Physics and International Center for Quantum Structures, Institute of Physics, Chinese Academy of Sciences, Beijing 100080, China*

[2]*Steacie Institute for Molecular Sciences, National Research Council of Canada, Ottawa, Ontario, K1A 0R6, Canada*

[3]*Oak Ridge National Laboratory, Oak Ridge, Tennessee 37831-6032*

[4]*National Renewable Energy Laboratory, Golden, Colorado 80401*

(Received 28 September 2001; published 25 January 2002)

A method, by which periodic two-dimensional arrays of identical metal clusters of nanometer size and spacing could be spontaneously obtained by taking advantage of surface mediated clustering, is reported. The versatility of the method is demonstrated for a broad range of metals on Si(111)-(7 × 7) substrates. *In situ* scanning tunneling microscopy analysis of In clusters, combined with first-principles total energy calculations, unveils unique initial-stage atomic structures of the surface-supported clusters and the vital steps that lead to the success of this method. A strong interaction between the clusters and the surface holds the key to the observed cluster sizes.

DOI: 10.1103/PhysRevLett.88.066101 PACS numbers: 81.07.–b, 07.79.Cz, 61.46.+w, 68.43.Bc

Ordered arrays of metal nanoclusters are promising materials for next generation microelectronics [1,2], ultra-high-density recording [3], and nanocatalysis [4,5]. Self-organization in heterogeneous strained thin-film growth [6,7] and self-assembly in chemical synthesis [3] are two of the most commonly used methods to obtain such nanostructures spontaneously. No method has succeeded in producing reproducibly identical nanoclusters/dots with periodic spatial distribution, which is highly desirable for practical device applications and is an open question in molecular and solid-state physics of these "artificial atoms" [8]. Fabrication of uniform-size cluster arrays at the ultrasmall 1–2 nm size regime is even more challenging because fluctuation at a level of only a few atoms could substantially alter their electronic properties. On the other hand, ultrasmall cluster arrays of such dimension have potential for quantum application because the Fermi wavelength for most metals is around 1 nm. At such a length scale, one could also maximize quantum confinement effects and test the fundamental limitations that such effects could impose on the electronic properties. Self-assembly of nanoclusters on periodic solid surface has been shown to be a promising approach to the problem [9–11], however, growth of ordered arrays of nanoclusters with identical size and tunable composition is still a daunting challenge.

Certain clusters with a specific (magic) number of atoms exhibit electronic and/or atomic closed-shell structures and hence remarkable stability [12]. For substrate-supported clusters, while the "closed-shell structure" is still under debate, several recent studies suggested that supported clusters of *specific* or "magic" sizes indeed exist with remarkable stability against others [13–16]. As the substrate could interact with the clusters, a substrate modification of the magic sizes may be unavoidable. On the other hand, such an interaction could play a pivotal role by automatically selecting identically sized clusters that for gas phase has to be done by mass spectrometry. Here, we explore this concept and exploit the magic clustering process to assemble ordered cluster arrays. We show that *substrate-induced spontaneous clustering* can be realized by delicate control of growth kinetics [17], and that periodic identical-size metal nanocluster arrays can be fabricated on Si(111)-(7 × 7) surfaces.

Our experiments were performed with a OMICRON variable temperature STM operated in ultrahigh vacuum ($\sim 5 \times 10^{-11}$ Torr). Clean Si(111) substrates were prepared by standard annealing procedures. Boron nitride crucibles were used to produce In (purity 99.999 99%) atomic beams, while Ag and Mn depositions were performed by resistant heating in a tungsten bracket filament and a tantalum boat, respectively.

Delicate regulation of the growth parameters allows for the growth of periodically ordered nanocluster arrays on the Si(111) substrate. Taking the In clusters in Fig. 1(a) as an example, even at 0.05 ML coverage a local ordering is already evidenced and all of them occupy the faulted half unit-cells (FHUCs) of Si(111)-(7 × 7) [18,19]. Also, the nanoclusters show high uniformity: every cluster in Fig. 1(a) is exclusively imaged as a hollow-centered, six-spot equilateral triangle. At a coverage of 0.12 ML, a perfectly ordered nanocluster array forms with a nearest neighbor distance of 2.7 nm [Fig. 1(b)]. With increasing In coverage, the clusters begin to occupy the unfaulted half unit cells (UFHUCs) of the surface without damaging the existing clusters on the FHUCs, which is different from the Tl case [9]. These clusters exhibit the same appearance as those in the FHUCs [Fig. 1(a)]. At ~0.24 ML, a characteristic ordered honeycomb structure develops (not shown), due to full occupation of both halves of the unit cell.

The general applicability of the method has been demonstrated by growing more than 12 ordered arrays of

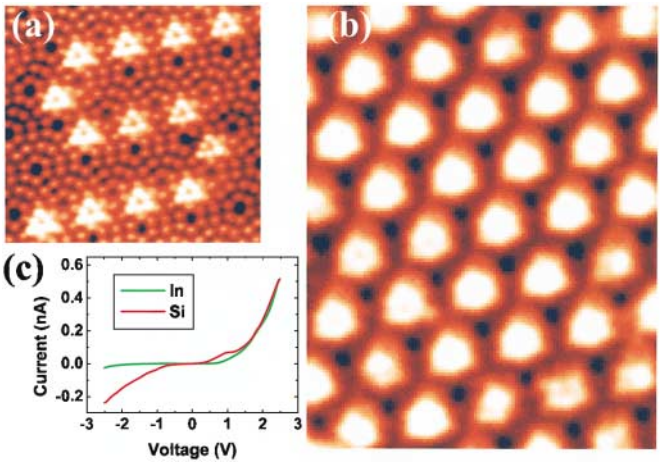

FIG. 1 (color). (a) STM image of In nanoclusters on Si(111) at an In coverage of ~0.05 ML (1 ML = one adsorbed atom per substrate atom). (b) Perfectly ordered In nanocluster arrays at ~0.12 ML In coverage. (c) *I-V* curves measured on bare Si surface (red) and on top of In clusters (green).

identical-size nanoclusters with different metals. An interesting example is the ordered arrays of even *complex* nanostructures. Here, the chemical identity of the STM image features can be determined by tracing deposition history. The complex array in Fig. 2(a) consists of two equivalent In and Mn cluster triangular lattices occupying, respectively, the FHUCs and UFHUCs, formed by depositing ~0.1 ML Mn on the In covered surface shown in Fig. 1(b). If ~0.06 ML Ag rather than Mn is deposited, an array of identical-size In/Ag alloy clusters forms. In this case [Fig. 2(b)], the subsequently deposited Ag atoms sit on top of the predeposited, ordered In clusters, rather than on the UFHUCs. The In cluster array therefore dictates the growth of the Ag cluster array. This salient feature is best illustrated at lower In/Ag coverage where the magic In clusters appear as a three-spot triangle indicated by the yellow triangle in Fig. 2(c). In contrast, the In/Ag binary clusters show four-spot triangles (with one spot at the center) as typified by the dark-blue triangle in Fig. 2(c). *In situ* Auger electron spectroscopy measurement shows the presence of Ag on the surface. Hence the center spots can be assigned to the tunneling current from the later-deposited Ag atoms.

Because the physical properties of the nanostructures are both size and material specific, and the cluster size and their array periodicity are comparable to the Fermi wavelengths of electrons in most metals, this method renders the potential to fabricate "customized" quantum devices. We note that (i) all the ordered cluster arrays shown here are stable with temperatures up to 200 °C. This feature is to be contrasted with metal clusters on metal surfaces, which are typically stable only at low temperatures [e.g., up to 150 K for Ag clusters on Pt(111) [7]. (ii) There is no fundamental limitation on fabricating identical-size clusters, as identical size has been demonstrated for In/Ag in Fig. 2(b). Thus, upon further improvement the present approach can be made precise and practical in fabricating various identical-size cluster arrays. We emphasize that our approach is not limited to Si. It applies as long as the substrate template used to accumulate and separate these building blocks exists or can at least be prepared. The $Si_3N_4(0001)$-(8×8) surface is among the candidate templates [20].

To understand the basic principles governing the array formation process, we have studied in some detail the atomic structures of the In clusters. The In clusters are an important component in Fig. 2 and in many aspects the most interesting. This is evidenced by the high-resolution STM images in Figs. 1(a) or 3(b) in which the In clusters appear as hollow-centered six-spot equilateral triangles. The triangular pattern is quite unusual in terms of normal close-packed structures [13,14,21]. An intuitive interpretation of the images could be that each bright spot of the triangle represents an In atom, which agrees with In coverage calibration in our experiment. However, the open triangular geometry seems to be unstable in view of the loose packing, the low coordination number, and in particular the strong steric strain with registry to atoms on the Si substrate. Alternatively, one might attribute the six spots seen to a dynamical time averaging of more than six atoms [9]. It was recently

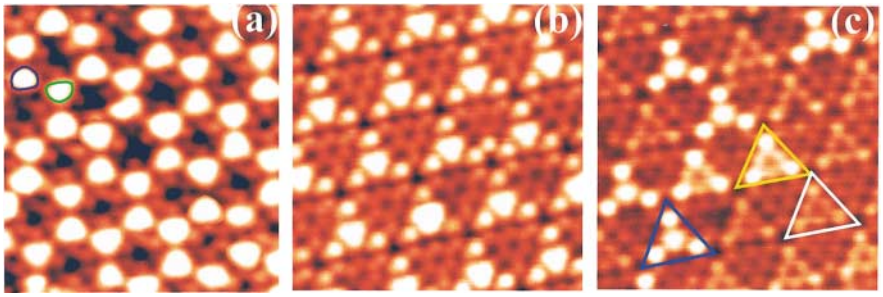

FIG. 2 (color). (a) Mixed array of equal-size In and Mn clusters formed by depositing ~0.1 ML Mn on preexisting array of In clusters shown in Fig. 1(b). The blue half circle highlights the In cluster, while the light green half circle highlights the Mn cluster. (b) Identical In/Ag alloy cluster array prepared by depositing ~0.06 ML Ag atoms (~three Ag atoms per unit cell) on the In cluster array shown in Fig. 1(b). (c) STM image for the surface with low In/Ag coverage, demonstrating that the nanoclusters in (b) are In/Ag alloy. The FHUC of the Si(111)-(7×7) is highlighted by a white triangle, whereas these occupied by pure In cluster and by mixed In/Ag cluster are highlighted by a yellow and a dark-blue triangle, respectively.

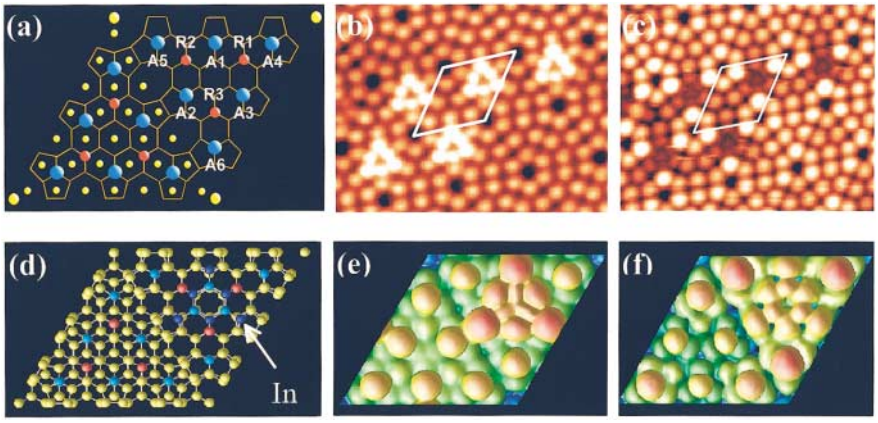

FIG. 3 (color). (a) The dimer-adatom-stacking-fault model of Si(111)-(7 × 7) surface (Ref. [18]). The FHUC is to the upper-right corner. The sites relevant to the discussion are indicated as $R1$-$R3$ for Si rest atoms and $A1$-$A6$ for Si adatoms. The yellow balls are Si atoms in the substrate, the blue balls are Si adatoms, and the red balls are Si rest atoms. (b) and (c) The STM images of the In clusters recorded at sample bias voltages of +0.6 and −0.3 V, respectively. (d) Top view of the calculated atomic structure of the six-In cluster on Si(111)-(7 × 7). The dark-blue balls are In atoms. The calculated STM images are shown in (e) (for positive bias +0.6 V) and (f) (for negative bias at −0.3 V with respect to the Fermi energy) for the atomic structure in (d). The colors indicate the height of the images: dark blue being low and red being high. At typical experimental tip height of about 1 nm above the surface, only the most protruding features can be seen.

shown that the potential energy surface of a Si adatom on Si(111)-(7 × 7) is quite shallow [22]. Therefore, it is possible that at room temperature In atoms may hop quickly along the local energy minimum sites [9] within the basin formed by one Si rest-atom and three Si adatoms [Fig. 3(a)], and the six bright spots reflect these energy minimum sites with higher occupation probability. This possibility, however, can be ruled out because our STM experiment at ~30 K shows exactly the same six-spot pattern. Furthermore, this model fails to account for the observed orientation of the triangles.

To address these puzzling issues, we carried out first-principles total energy calculations. A Vanderbilt ultrasoft pseudopotential [23] was used with a 100 eV cutoff energy and 1 special k point in the Brillouin zone sum. The bare 7 × 7 unit cell (without counting the Si adatoms) contains six Si layers and a vacuum layer equivalent to six Si layers. We calculated the STM images following the Tersoff and Hamann formula [24] as detailed in Refs. [25,26].

Two possible In-cluster structures are considered: (i) six-In-atom cluster forming a hexagonal ring; (ii) six-In-atom cluster forming a hollow-center triangle. In case (i), each of the six In atoms is bonded to either one of the three Si adatoms ($A1$-$A3$) or one of the three Si rest atoms ($R1$-$R3$) [Fig. 3(a)]. The In atoms are also bonded among themselves forming a distorted hexagonal ring. This model cannot explain the STM images, in particular the image for the filled states [Fig. 3(c)]. Its energy is also 1.2 eV/cluster higher than case (ii). In case (ii), six threefold-coordinated In form a triangle [Fig. 3(d)]. For In atoms at the corners of the triangle, the bond lengths are 2.57, 2.64, and 2.64 Å, whereas the bond angles are 113°, 113°, and 88°, respectively. For In atoms on the edges, the bond lengths are 2.67, 2.60, and 2.60 Å, whereas the bond angles are 113°, 116°, and 116°, respectively. Angles larger than the 109.5°-tetrahedral angle are preferential as threefold In prefers planar 120° bond angles. Both the three Si adatoms ($A1$-$A3$) and the three Si rest atoms ($R1$-$R3$) become fourfold coordinated. Noticeably, Si adatoms $A1$-$A3$ are displaced towards the triangle center considerably, which strengthens their bonds with the substrate atoms by resuming the 109.5°-tetrahedral angles. Each Si adatom has two 80°, one 83°, and three close-to-tetrahedral angles. Similar geometries have been suggested for low energy defects in hydrogenated Si [27] and for the DX center in III-V alloys [28]. Thus, by displacing Si adatoms not only can the perceived steric strain be avoided, but also the displaced Si adatoms serve as the "missing" links between the otherwise loosely packed In atoms. An In cluster on the UFHUC is found to be 0.1 eV/cluster higher in energy than that on the FHUC.

The atomic registry of the In cluster in Fig. 3(d) further explains why the number six is so special or magic, as either addition or removal of one In atom will destabilize the cluster. The same argument applies to larger clusters, but will not be discussed here. Our results suggest that local optimization of the chemical bonds is essential for the exceptional stability of the magic clusters. The energy barrier for the In atoms to reach their optimal positions is expected to be only moderate as the cluster formation involves only the insertion of In into the existing 7 × 7 surface network that is quite flexible compared to bulk. Massive rearrangement of the surface should be avoided, as it will lead to $\sqrt{3} \times \sqrt{3}$ or other structures [29].

The calculated STM images in Figs. 3(e) and 3(f) are in remarkable qualitative agreement with experiment [Figs. 3(b) and 3(c)]. Interestingly, in the empty state image [Fig. 3(e)], the three brightest spots are from the lowest In atoms, which are 0.6 Å lower than Si $A1$−$A3$ with an average bond angle of 105° (thus sp^3-like). The

three second-brightest spots are from the other In atoms, which are 0.3 Å lower than Si $A1$-$A3$ with an average bond angle of 115° (thus sp^2-like). Si adatoms $A1$-$A3$ are almost invisible, as they do not involve any dangling bond. A large disparity between an STM image and actual height of group III atoms has been demonstrated for an As vacancy on GaAs(110) surface [25]. Another striking feature in Fig. 3(c) is the disappearance of the six-In triangle spots under small *reverse* bias, whereas the three Si corner adatom spots ($A4-A6$) become significantly brighter. Our calculation reveals that this change is not due to In diffusion but has an electronic origin. The calculated density of states reveals a 0.33 eV band gap 0.2 eV below the Fermi energy (E_F). States below the gap have mainly the Si/In bonding character. States above the gap but below E_F have mainly the dangling-bond character and are predominantly on Si $A4-A6$. The In dangling bond states are found to be *above* E_F thus can only be seen in the empty state image. A micro C-V profile above In clusters should unveil this semiconducting characteristics. Indeed, this is confirmed in our experiment [Fig. 1(c)] and by others [30].

Our discussion hereto suggests that while the clusters are locally stable, globally they are metastable. Then, what has led to the success of the current approach while it has not been possible in the past? Our experiment demonstrates that it needs delicate control of the growth kinetics [17]. (i) One must suppress the formation of any undesirable clusters of inhomogeneous sizes. If the substrate temperature during deposition is too low (room temperature or lower) and the deposition rate is too high, the In atoms do not have enough time to arrive at the expected destination as required for the formation of stable clusters. Instead, they combine to form immobile nuclei of smaller sizes. "Hot-landing" at high temperatures would allow energetic In atoms to agglomerate into larger clusters which then coalesce into islands via Ostwald ripening, or phase transition into the $\sqrt{3} \times \sqrt{3}$ structure. (ii) The calculated energy difference between In clusters on the FHUC and UFHUC is only 0.1 eV/cluster. Given such a modest energy difference, the kinetics have to be manipulated in such a way that the atom hopping rate between the two halves must exceed the atom arrival rate enough to complete the ordering. To achieve such balance, we find that the substrate temperature during deposition should be higher than 100 °C but lower than 200 °C while the deposition rate should be around 0.01 ML/min for In, Ag, and Mn.

In summary, we have demonstrated an efficient method for fabricating "customized" highly uniform nanocluster arrays on Si(111) with atomic precision. The physical origin of the stable or magic sizes that makes the method possible is established and the atomic structures for the In clusters are determined by first-principles calculations. The ability to assemble nanoclusters and the thermal stability up to 200 °C for the nanocluster arrays on Si allow for integration with existing microelectronic architectures. Finally, the ability to form magnetic and/or alloyed nanocluster arrays may lead to breakthroughs in other important areas such as surface nanocatalysis [4] and nanomagnetism [5].

S. B. Z. thanks W. E. McMahon for a critical reading of the manuscript. Work at IOP was supported by the NSF of China (69625608), at NREL by the U.S. DOE/SC/BES under Contract No. DE-AC36-99GO10337 and by the U.S. DOE/NERSC for supercomputer time, and by Oak Ridge National Laboratory, managed by UT-Battell, LLC for the U.S. DOE under Contract No. DE-AC05-00OR22725, and by the U.S. NSF (DMR-0071893), respectively.

[1] A. O. Orlov *et al.,* Science **277**, 928 (1997).
[2] R. P. Andres *et al.,* Science **272**, 1323 (1996).
[3] S. Sun *et al.,* Science **287**, 1989 (2000).
[4] M. Valden, X. Lai, and D. W. Goodman, Science **281**, 1647 (1998).
[5] M. Haruta, Catal. Today **36**, 153 (1997).
[6] K. Bromann *et al.,* Science **274**, 956 (1996).
[7] H. Brune *et al.,* Nature (London) **394**, 451 (1998).
[8] P. L. McEuen, Science **278**, 1729 (1997).
[9] L. Vitali, M. G. Ramsey, and F. P. Netzer, Phys. Rev. Lett. **83**, 316 (1999).
[10] J. Myslivecek *et al.,* Phys. Rev. B **63**, 045403 (2001).
[11] M. Yoon *et al.,* Phys. Rev. B **64**, 085321 (2001).
[12] W. D. Knight *et al.,* Phys. Rev. Lett. **52**, 2141 (1984).
[13] D. M. Chen *et al.,* Phys. Rev. Lett. **61**, 2867 (1988).
[14] M. Y. Lai and Y. L. Wang, Phys. Rev. Lett. **81**, 164 (1998).
[15] F. Liu *et al.,* Chem. Phys. Lett. **248**, 213 (1996).
[16] K-J. Jin *et al.,* Phys. Rev. Lett. **80**, 1026 (1998).
[17] Z. Zhang and Max. G. Lagally, Science **276**, 377 (1997).
[18] K. Takayanagi *et al.,* J. Vac. Sci. Technol. A **3**, 1502 (1985).
[19] G.-X. Qian and D. J. Chadi, Phys. Rev. B **35**, 1288 (1987).
[20] X.-S. Wang *et al.,* Phys. Rev. B **60**, R2146 (1999); H. Ahn *et al.,* Phys. Rev. Lett. **86**, 2818 (2001).
[21] I.-S. Hwang, M.-S. Ho, and T. T. Tsong, Phys. Rev. Lett. **83**, 120 (1999).
[22] K. Cho and E. Kaxiras, Surf. Sci. **396**, L261 (1998).
[23] D. Vanderbilt, Phys. Rev. B **41**, 7892 (1990).
[24] J. Tersoff and D. R. Hamann, Phys. Rev. B **31**, 805 (1985).
[25] S. B. Zhang and A. Zunger, Phys. Rev. Lett. **77**, 119 (1996).
[26] T. Hitotsugi *et al.,* Phys. Rev. Lett. **82**, 4034 (1999).
[27] R. Biswas and Y.-P. Li, Phys. Rev. Lett. **82**, 4034 (1999).
[28] S. B. Zhang and D. J. Chadi, Phys. Rev. B **42**, 7174 (1990).
[29] J. Kraft, M. G. Ramsey, and F. P. Netzer, Phys. Rev. B **55**, 5384 (1997).
[30] X. F. Lin *et al.,* J. Vac. Sci. Technol. B **14**, 995 (1996).